DC TRANSMISSION NETWORKS

A number of high-voltage direct-current (HVDC) links are functioning within the existing ac transmission systems in many countries, and the option of including multiterminal dc subnetworks is receiving considerable attention. HVDC transmission subsystems are preferred for better economic and technical benefits in specific applications, such as

- To transfer bulk load over long distance more economically
- To transmit power in underground and submarine cables
- To facilitate the operation of interconnected ac systems at different frequencies
- To reduce the short-circuit level in an interconnected ac system
- To increase the transient stability margin
- To improve the dynamic stability

Load flow is an important part of power system planning and operation. Many papers have been published on ac–dc load flow (1–6). Different types of algorithms have been proposed (1–7). However, most of these studies have been carried out on ac–dc systems, and no generalized dc transmission papers have been found in the literature. Most of the work have been carried out for specific application (8,9).

An inspection of the available literature indicates that practically adopted ac–dc load flow algorithms are based on either Newton–Raphson (NR) or the fast decoupled (FD) technique. Stott (2) combined the dc link solution technique of Sato and Arrillaga (3) with the NR ac load-flow program and solved the ac–dc load-flow problem in the sequential framework. The FD load-flow scheme was extended to the ac–dc load flow by Arrillaga, Bodger, and Harker (4), El-Marsafawy and Mathur (5), and many others. However, the algorithms presented in Refs. 4 and 5 using the simultaneous solution scheme are computationally superior, practically viable, and technically versatile. All the previous discussions are pertinent to ac–dc load-flow only. The proposed technique can faithfully be applied to ac systems, dc networks, and ac–dc (interface) systems.

PROBLEM FORMULATION

In this section a mathematical model for dc transmission network and ac–dc systems is developed. An integrated ac–dc system consists of ac network, dc network, and ac–dc interface (converter) system. For the purpose of dc transmission network analysis, ac network components connected to a converter are considered as part of the converter system. The advantage of this approach is that the ac network admittance matrix remains unaffected due to converter transformer tap variations or due to reactive power changes caused by switching of the capacitor banks at the converter terminal busbars.

DC CONVERTER AND NETWORK MODEL

For the purpose of analysis of dc transmission networks, HVDC converters have, so far, been modeled in polar coordinate form. In this section, the HVDC converters are modeled in the rectangular coordinate form. A HVDC converter connected to an ac busbar P and a dc busbar i is shown in Fig. 1.

For the purpose of the mathematical model the following simple assumptions are made:

- The three-phase voltage at a converter terminal busbar is balanced and sinusoidal at system frequency.
- Converter valves are ideal (no voltage drop) and converter operation is balanced.
- Converter transformer is lossless and its magnetizing admittance is negligible.
- Dc voltages and currents are smooth (ripple-free).

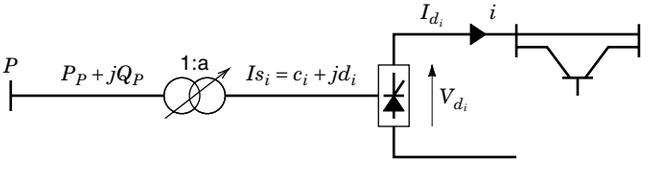

Figure 1. HVDC converter and network model.

- The effect of the overlap angle (μ) while establishing a relationship between the secondary current of the converter transformer and converter current is neglected.

These assumptions are reasonable and made for the polar coordinate formulation as well.

MATHEMATICAL MODEL FOR RECTANGULAR COORDINATES

The performance equations using the converter variables in the rectangular coordinates are derived and are as follows: The dc voltage V_{d_i} at the converter terminal i is

$$V_{d_i} = k_1 a_i \cos\theta_i |V_P| - S_i k_2 X_{c_i} I_{d_i} \tag{1}$$

where $k_1 = 3\sqrt{2/\pi}$, a_i is the converter transformer tap, θ_i is the converter control angle,

$$\theta_i = \begin{cases} \alpha_i & \text{for rectifier operation} \\ \lambda_i & \text{for inverter operation} \end{cases}$$

V_P is the ac terminal voltage, S_i

$$S_i = \begin{cases} 0 & \text{if no converter at ac busbar} \\ 1 & \text{if converter at ac busbar P is a rectifier} \\ -1 & \text{if converter at ac busbar P is an inverter} \end{cases}$$

$k_2 = 3/\pi$, X_{c_i} is the commuting reactance, and I_{d_i} is the dc current.

Expressing V_p in rectangular coordinates,

$$V_{d_i} = k_1 a_i \cos\theta_i (e_P^2 + f_P^2)^{1/2} - S_i k_2 X_{c_i} I_{d_i} \tag{2}$$

Squaring both sides and rearranging Eq. (2) can be written as

$$(k_1 a_i \cos\theta_i)^2 (e_P^2 + f_P^2) - (V_{d_i} + S_i k_2 X_{c_i} I_{d_i})^2 = 0 \tag{3}$$

The complex power injection ($P_P + jQ_P$) into the HVDC converter at ac terminal busbar P is

$$P_P + jQ_P = S_i V_P I_P^* = S_i a_i V_p I_{s_i}^* \tag{4}$$

where I_p is the primary side current and I_{s_i} is the secondary side current, $I_{s_i} = c_i + jd_i$.

Expressing V_P and I_{s_i} in rectangular coordinates,

$$P_P + jQ_P = S_i a_i [(e_P c_i - f_P d_i) + j(e_P d_i + f_P c_i)] \tag{5}$$

The real power P_P from Eq. (5) is

$$P_P = S_i a_i (e_P c_i - f_P d_i) \tag{6}$$

Neglecting losses in the converter and converter transformer, the following relationship holds:

$$P_{ac} = P_{dc} \tag{7}$$

Therefore, the real power injection into the HVDC converter in terms of the dc voltage and current is

$$P_P = V_{d_i} I_{d_i} \tag{8}$$

From Eqs. (6) and (8)

$$V_{d_i} I_{d_i} - S_i a_i (e_P c_i - f_P d_i) = 0 \tag{9}$$

The dc current injection at the dc busbar i in terms of dc network conductance and dc busbar voltage is

$$I_{d_i} = \sum_{j=1}^{N_{dc}} G_{dc_{ij}} V_{d_j} \tag{10}$$

Rearranging Eq. (10)

$$I_{d_i} - \sum_{j=1}^{N_{dc}} G_{dc_{ij}} V_{d_j} = 0 \tag{11}$$

The secondary current of the converter transformer is related to the dc current as shown in Eq. (12) is

$$k_1 I_{d_i} = |I_{s_i}| = (c_i^2 + d_i^2)^{1/2} \tag{12}$$

Squaring both sides of Eq. (12) and after arranging

$$(k_1 I_{d_i})^2 - (c_i^2 + d_i^2) = 0 \tag{13}$$

For a HVDC converter operating under the balanced condition from a known ac terminal voltage, only two independent variables V_d and I_d are sufficient. However, the control requirements of the converter involve additional variables. In the rectangular coordinate formulation, a set of six variables (V_d, I_d, a, c, d, cos θ) are required for the modeling of the HVDC converter. Whereas in the polar coordinate formulation, five variables (V_d, I_d, a, ϕ, cos θ) are sufficient. In the latter case the converter secondary current angle is taken as shown in Ref. 2. The choice of cos θ instead of θ as a primary dc variable removes the trigonometric nonlinearity from the system equations.

The evaluation of the six variables of the converter model in the rectangular coordinate requires six independent equations. Of the six, four equations are characterized by the mathematical model as expressed in Eqs. (3), (9), (11), and (13). The other two independent equations are obtained from the specified control strategy for the converter operation.

The converter controls normally specified are

1. Specified dc voltage:

$$V_{d_i} - V_{d_i}^{sp} = 0 \tag{14}$$

2. Specified dc current:

$$I_{d_i} - I_{d_i}^{sp} = 0 \tag{15}$$

3. Specified dc power:

$$P_{d_i} - P_{d_i}^{sp} = 0 \tag{16}$$

Table 1.

	V_d	I_d	a	c	d	θ
Converter 1	1.29577	0.44835	0.97428	8.499	0.56905	0.20174
Converter 2	1.27950	−0.55029	1.03619	19.998	0.62789	0.39020
Converter 3	1.28891	0.10080	0.98398	12.498	0.12591	0.05015

4. Specified firing angle θ:

$$\cos\theta_i = \cos\theta_i^{\text{sp}} = 0 \tag{17}$$

5. Specified converter transformer tap position:

$$a_i - a_i^{\text{sp}} = 0 \tag{18}$$

6. Specified converter reactive power:

$$a_i(e_{\text{P}}d_i + f_{\text{P}}c_i) - Q_i^{\text{sp}} = 0 \tag{19}$$

These control equations are simple and easily incorporated into the solution algorithm.

The *P–V*, *P–I*, and *V–I* controls, being overspecified, are normally not used. For the load-flow analysis, the mathematical model of a HVDC converter is written in the residual form. The residual in the concise form is

$$[\overline{Xd}, \overline{e}, \overline{f}] = 0 \tag{20}$$

where

$$\begin{aligned}
\Delta R_{i1} &= (k_1 a_i \cos\theta_i)^2(e_{\text{P}}^2 + f_{\text{P}}^2) - (V_{\text{d}_i} + S_i k_2 X_{\text{c}_i} I_{\text{d}_i})^2 \\
&\quad \text{from Eq. (3)} \\
\Delta R_{i2} &= V_{\text{d}_i} I_{\text{d}_i} - S_i a_i (e_{\text{P}} c_i - f_{\text{P}} d_i) \quad \text{from Eq. (9)} \\
\Delta R_{i3} &= I_{\text{d}_i} - \sum_{j=1}^{Nac} G dc_{ij} V d_j \quad \text{from Eq. (11)} \\
\Delta R_{i4} &= (k_i I d_i)^2 - (c_i^2 + d_i^2) \quad \text{from Eq. (13)} \\
\Delta R_{i5} &= \text{control equation} \\
\Delta R_{i6} &= \text{control equation}
\end{aligned} \tag{21}$$

where $G_{\text{dc}_{ij}}$ is the (i, j)th element of the dc network conductance matrix and N_{dc} is the number of dc busbars.

Six equations similar to Eq. (21) are written for each converter. Such equations for all converters characterize the mathematical model of a dc system.

RESULTS

An exhaustive simulation have been carried out on the IEEE 14-, 30- and 57-busbar systems. In an actual ac system some busbars are modified to dc and to form either a mesh or link or mesh-link system. The actual formation of these lines are explained in Ref. 6. Some dc results of the IEEE 30-bus system with a dc mesh-link system is provided in Table 1. The test results are found to be in good agreement.

CONCLUSIONS

A dc transmission system is usually incorporated into an electric power system because of special and unique reasons that are not adequately or economically served by ac transmission. Variables of the dc link that have been chosen for the problem formulations are the converter transformer tap ratio, converter terminal, firing angle of the rectifier, commutating reactance, dc voltage and the current in the dc link. Equations relating these six variables and their solution strategy have been discussed. The model developed is independent of a particular control of the dc link.

BIBLIOGRAPHY

1. J. Arrillaga, P. Bodger, and B. J. Harker, FDLF algorithm for ac-dc system, *IEEE PES Summer Meeting,* Los Angeles, 1978, paper A 78, 555-5, pp. 16–21.
2. B. Stott, *Load flow solution for ac and integrated ac-dc power system,* Ph.D. thesis, Victoria Univ. of Manchester, 1971.
3. H. Sato and J. Arrillaga, Improved load flow techniques for integrated ac-dc system, *Proc. IEE,* **116**: 525–532, 1969.
4. J. Arrillaga, P. Bodger, and B. J. Harker, FDLF algorithm for ac-dc system, *IEEE PES Summer Meeting,* Los Angeles, 1978, paper A-78, pp. 555–561.
5. M. M. El-marsafawy and R. M. Mathur, A new fast technique for load flow solution of integrated ac-dc system, *IEEE Trans. Power Appar. Syst.,* **PAS-99**: 246–255, 1980.
6. M. Z. Haque, *A sequential approach of solving second order ac-dc load flow and state estimation problems,* Ph.D. thesis, Victoria Univ. of Technol., Australia, 1996.
7. B. Stott and O. Alsac, Fast decoupled load flow, *IEEE Trans. Power Appar. Syst.,* **PAS-93**: 859–869, 1974.
8. E. L. Hjort and Tommy, Direct current distribution line installed in Sweden, *Transmission Distrib. World,* **49**: 80–83, 1997.
9. N. G. Hingorani, High voltage dc transmission: A power electronics workhouse, *IEEE Spectrum,* **33** (4): 63–72, 1996.

ZAHIDUL HAQUE
AKHTAR KALAM
Victoria University of Technology

DEBUGGING. See SOFTWARE BUGS.

DEBUGGING PARALLEL PROGRAMS. See PARALLEL PROGRAMMING TOOLS.

DECENTRALIZED CONTROL. See LARGE-SCALE AND DECENTRALIZED SYSTEMS.

DECIDABILITY. See COMPUTABILITY.

DECISION ANALYSIS. See OPERATIONS RESEARCH DECISION MAKING.

DECISION LOGIC. See MAJORITY LOGIC.

DECISION MAKING. See OPERATIONS RESEARCH DECISION MAKING; PROBABILISTIC RISK ASSESSMENT.

DECISION SYSTEM FOR ROBOT SELECTION. See EXPERT DECISION SYSTEM FOR ROBOT SELECTION.